Macromolecules

ARTICLE

pubs.acs.org/Macromolecules

4,4′,4″-Tris(acetoxymethylene)triphenylamine: An Efficient Photoacid Promoted Chemical Cross-Linker for Polyvinylcarbozole and Its Applications for Photolithographic Hole-Transport Materials

Yu-Xun Wang and Man-kit Leung*

Department of Chemistry and Institute of Polymer Science and Engineering, National Taiwan University, 1, Roosevelt Road Section 4, Taipei, Taiwan 106, ROC

Supporting Information

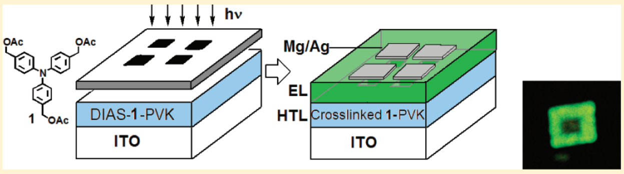

ABSTRACT: A photolithographic hole transport material of 4,4′,4″-tris(acetoxymethylene)triphenylamine (**1**), polyvinylcarbazole (PVK), and diphenyliodonium 9,10-dimethoxyanthracene-2-sulfonate (DIAS, a photoacid generator) has been successfully formulated. After exposure to UV irradiation ($\lambda > 200$ nm) through a patterned UV ($\lambda > 200$ nm) photomask for 6 min, followed by a standard postbaking treatment at 130 °C for 5 min under vacuum and development in CH_2Cl_2, a negative tone image was established through the photoinduced chemical cross-linking reactions. This approach can be implemented to PLED applications. Under the optimized conditions, the polymeric light-emitting device (PLED) of ITO/photolithographic HTL/PVK−Ir(PPy)$_3$−PBD/Mg−Ag, with a turn-on voltage of 13.0 V (100 cd/m^2), a maximum brightness of 8220 cd/m^2, and a current efficiency of 9.0 cd/A was achieved. Our study reviewed that three parallel mechanisms, including the photodimerization of the carbazole units, the Crivello onium salt sensitization mechanism, and the photoacid catalyzed Friedel−Crafts type electrophilic aromatic substitutions are involved in the photocross-linking process.

INTRODUCTION

Organic light-emitting diodes (OLEDs) are "dual-injection" devices in which holes and electrons are injected and transported respectively from two opposite electrodes, recombining to generate excitons that emit light in the light-emitting zone.[1] To obtain a highly efficient device, the recombination zone has to be kept away from the electrode surface in order to avoid the exciton-quenching. In principle, the structure of the OLED could be as simple as a single layer device, provided that the both carrier-fluxes are all balanced.[2] However, for most organic materials, these requirements are too vigorous to fulfill. Therefore, multilayer structures were developed for typical OLED applications, in which discrete hole-transport, light emitting, as well as electron-transport layers are sequentially constructed between the cathode and anode through high vacuum vapor deposition conditions.[3] In these devices, generation of excitons is confined within the light-emitting layer (EL) so that device efficiency could be optimized.

Instead of using the vapor deposition approach, polymeric optoelectronic devices could be usually fabricated through the layer by layer spin-coating or dip-coating techniques.[4] However, swelling or redissolution of the precoated layers from substrate might occur during the sequential coating process, and thus lead to the destruction of the device structures. Therefore, various methods such as electrochemical, thermal, or photochemical cross-linking methods[5] have been developed to cross-link the precoated layers against solvent etching in the latter steps. For example, oxetane containing polymers have been used as the photocross-linkable hole-transport materials for PLED systems.[5d,e,k]

Lithography has been an important patterning technique for fabrication of integrated circuits.[6] To expand the scope of its applications, it is worthwhile to integrate organic semiconducting polymers with lithographic properties.[7] Because of the properties of organic polymers, including the band gap, absorption region, charge mobility, and conductivity, could be tuned through skeletal modification. Thus, a large variety of the electronic polymers with photolithographic properties could be developed. During the past few years, we are interested in hole-transport organic polymers.[8] In our recent research work, we have attempted to use triphenylamine (TPA) derivatives as cross-linkers to construct the photoimageable hole-transport layer (HTL).[8a]

TPA derivatives are good hole-transport materials due to their relatively high hole mobility (10^{-3}−10^{-4} cm·V·s^{-1}) and low ionization potentials.[9] The role of the HTL is not only to maximize hole-injection from the ITO anode, but also to act as a electron-blocking layer, preventing electron overflow from the EML so that it could confine excitons with the light emitting zone.[10] Recently, carbazole-based polymers using in light-emitting devices have attracted a lot of attention.[11] To be a good hole-transport material, many criteria such as high carrier mobility, thermal stability, and homogeneous morphology have to be

Received: August 9, 2011
Revised: September 28, 2011
Published: October 28, 2011

Scheme 1. Preparation of 1 from TPA

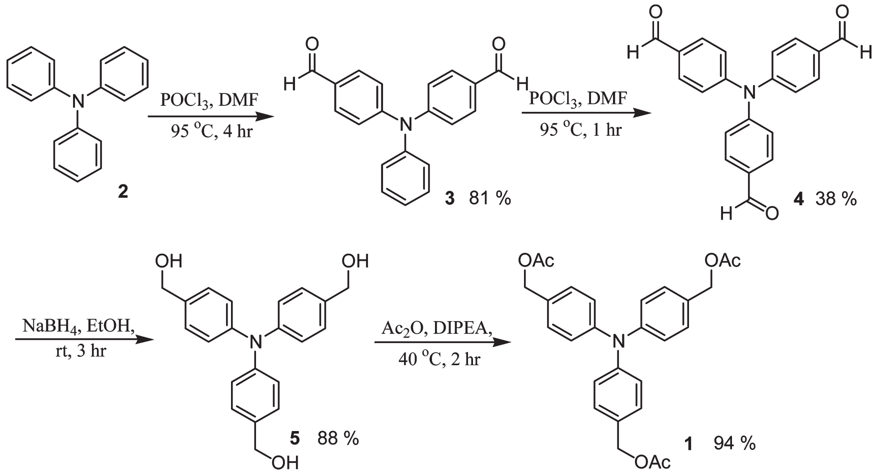

matched. In the present article, we report the use of **1** as a photocross-linker for polyvinylcarbazole (PVK) matrix, a commercially available material with wide applications. It was of interest whether cross-linking reaction would occur between **1** and PVK under UV-irradiation, or be promoted in presence of photo acid generator (PAG) to form insoluble polymer network. Furthermore, the possibility of generating patterned hole-transport layer onto the ITO substrate for PLED devices had been explored.

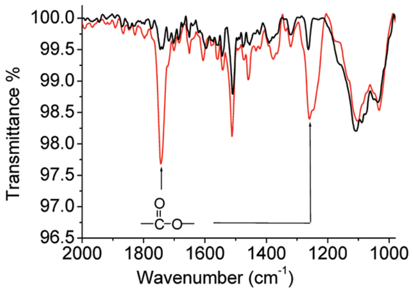

Figure 1. FT-IR spectra of **1**: (a) before (black line) and (b) after irradiation (red line).

RESULTS AND DISCUSSION

Preparation of 1. Starting from the commercially available TPA (**2**), we have first attempted using the Vilsmeier–Haack formylation[12] to prepare the trialdehyde **4**, but unsuccessfully, only resulting with the dialdehyde **3** as the major product, along with small amounts of the desired **4** being isolated (Scheme 1). This frustrating result may be due to the formation of the positively charged bis-iminium intermediate, which is strongly deactivating, prohibiting the intermediate from further imination process.[12] However, resubjecting the dialdehyde **3** back to the Vilsmeier–Haack conditions allowed the third formylation to go on to yield **4** that was reduced by using $NaBH_4$ to afford **5**. Finally, acetylation of **5** with acetic anhydride led to **1** in good yields.

Photochemical Response of 1. The photochemical activity of **1** was first monitored by using FT-IR spectroscopy. The light source being used for the photochemical study in the present work is a Xenon lamp (17 mW/cm^2) having a wavelength (λ) > 200 nm. However, the light source with the wavelength longer than 320 nm was found to be inactive and does not lead to any photochemical consequence after irradiation. Thin-film of **1** was prepared by spin-coating of the corresponding solution (5 mg/mL in $CHCl_3$) on a silicon wafer and dried at 80 °C for 5 min. The film thickness of 40 nm was recorded. Before irradiation, the FT-IR spectrum clearly shows vibrational absorption bands of the $-CO_2-$ group at 1258 and 1743 cm^{-1} respectively. After exposure to UV irradiation for 6 min and postbaking treatment at 130 °C for 5 min under reduced pressure, the absorption bands of the $-CO_2-$ group faded away in the IR spectrum (Figure 1), indicating that **1** could be photochemically decomposed. Further study revealed the IR intensity at 1258 and 1743 cm^{-1} drops significantly even before the sample being postbaked, indicating that the fading of the IR signals of the $-CO_2-$ group mainly occurred during the photoirradiation process. We tentatively proposed that **1** had been photodissociated under UV irradiation to release acetic acid that was further evaporated from the thin-film during the photoirradiation process and the postbaking heat treatment. The reaction mechanisms might involve either homolytic or heterolytic cleavage of the C–O bond. It is important to point out that only the heat treatment did not lead to any observable decomposition, indicating that exposure to UV-light is essential for promoting the photochemical decomposition process.

Photochemical Reactivity of 1 in CD_3OD. To get more insight about the photodecomposition of **1**, the photoirradiation was carried out in CD_3OD and the products being generated were directly examined by ^1H NMR spectroscopy. Figure 2 shows four sets of ^1H NMR signals at δ 7.24 (d, 2H), 6.98 (d, 2H), 5.04 (s, 2H), and 2.06 (s, 3H), which are assigned to H_a, H_b, H_c and H_d respectively. The sample is stable in CD_3OD and no methanolysis was observed after being heated in an oil bath at 50 °C for 2 h. However, photoirradiation under UV for 6 min led to partial decomposition that was clearly evidenced in the ^1H NMR spectrum (Figure 2b); new peaks were observed at δ 7.2, 7.0. 4.4, and 2.0 that are respectively assigned to $H_{b'}$, $H_{a'}$, $H_{c'}$, and the α-protons of acetic acid. Formation of acetic acid was evidenced by comparison the spectrum to that of the authentic sample (Figure S22, Supporting Information).

Photochemical Reactivity of 1 in PVK. According to the above IR studies, we concluded that **1** is photochemically active.

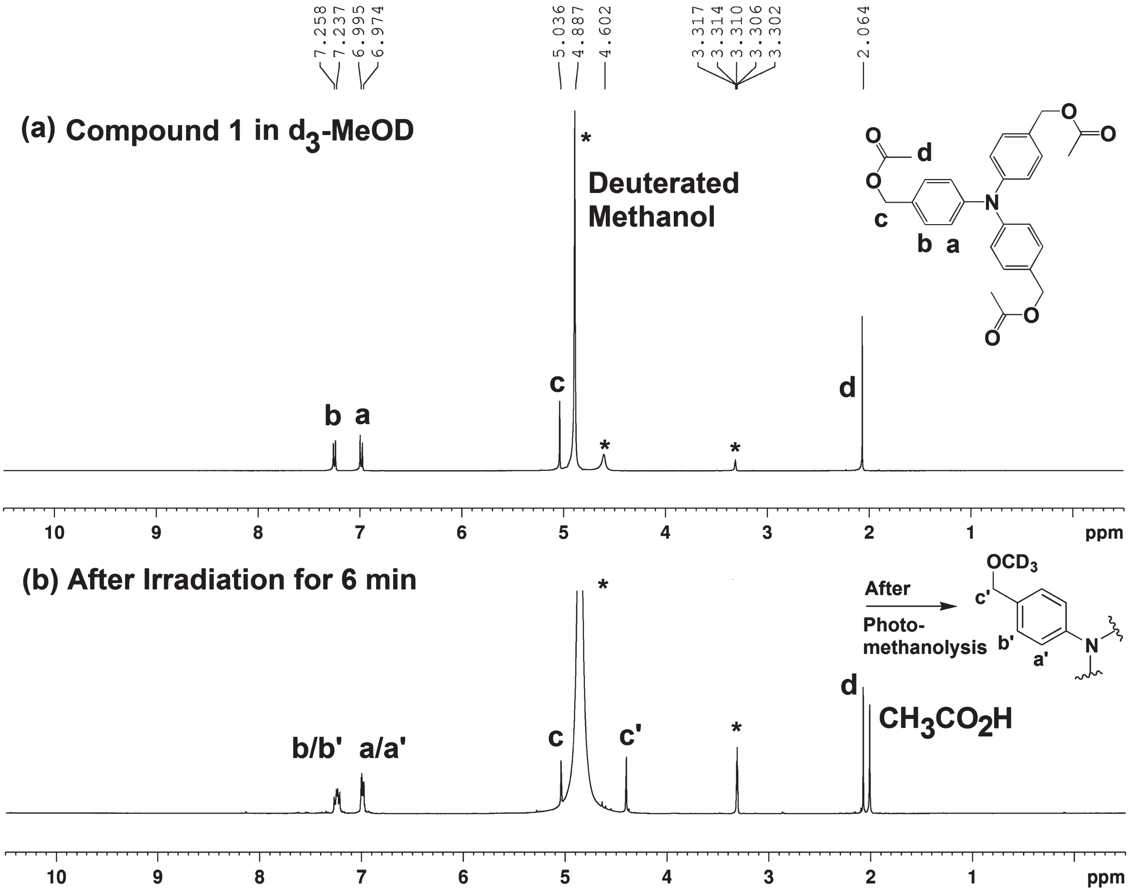

Figure 2. ^{1}H NMR trace of the photochemical reaction of **1** in methanol-d_4.

Therefore, we are curious to know if **1** could act as a useful photochemical cross-linker for PVK. Since PVK itself could be photochemically cross-linked under photoirradiation at the wavelength longer than 300 nm,[13] the background-control studies are also necessary in order to secure the conclusions.

In the following experiments, thin films were applied onto quartz substrates by spin-coating method, followed by UV curing and postbaking treatment as before. The layers being cured became partially insoluble. To monitor the degree of cross-linking, the cured films were developed by immersion in CH_2Cl_2 for 10 s. The soluble part would be dissolved into CH_2Cl_2 accordingly. The residual film thickness was analyzed by measuring their absorption intensity (I_R) at 345 nm. The intensity ratio of I_R/I_O, in which I_O is the original absorption intensity before irradiation, reflects the amounts of the residual film left on the substrate. The ratios of I_R/I_O from different film-compositions are summarized in Table 1.

In the first background-control study, we adopted a layer of pure PVK as our reference for UV-irradiation. The film was prepared from a solution of PVK in $CHCl_3$ (12.5 mg/mL). After irradiation and development, the average I_R/I_O value of 0.39 for the film at 345, 33, and 296 nm was obtained as shown in Figure 3a. The significant drop of the absorption intensity indicates that over 61% of the PVK has been dissolved and removed from the substrate during the development process. Although the observation of the photo-cross-linking phenomenon for PVK has been reported,[13,14] it is noteworthy to mention here about the degree of the photocross-linking which is apparently low and not enough to completely cross-link the film under our experimental conditions. Therefore, the PVK matrix was partially dissolved in the organic developer from the substrate.

Table 1. Photochemical Cross-Linking of PVK under UV Irradiation[a]

film	weight ratio	I_R/I_O		
		345 nm	331 nm	296 nm
PVK	pure	0.38	0.39	0.39
TPA-PVK	1:9	0.54	0.51	0.46
TriOAc-PVK	1:9	0.94	0.88	0.87
PAG-PVK	1:9	0.94	0.90	0.95
TriOAc-PAG-PVK	1:1:9	0.95	0.92	0.97

[a] With the wavelength >200 nm for 6 min.

Next experiment is to use a PVK-**1** blend as the photochemically active layer to study. Figure 3b shows the spectra of the films before and after UV irradiation and development. One can clearly see that two spectra almost overlay with each other. The high I_R/I_O value of 0.94 at 345 nm indicates that the film remains intact on the quartz substrate. This result implies that **1** plays a good role on cross-linking the PVK against the solvent etching during the development process. However, some spectral deviations at 331 and 296 nm, with the I_R/I_O values of 0.88 and 0.87 respectively, were observed. We attribute this to the partial leaching of the unbound **1** during development, leading to some loss of the optical density.

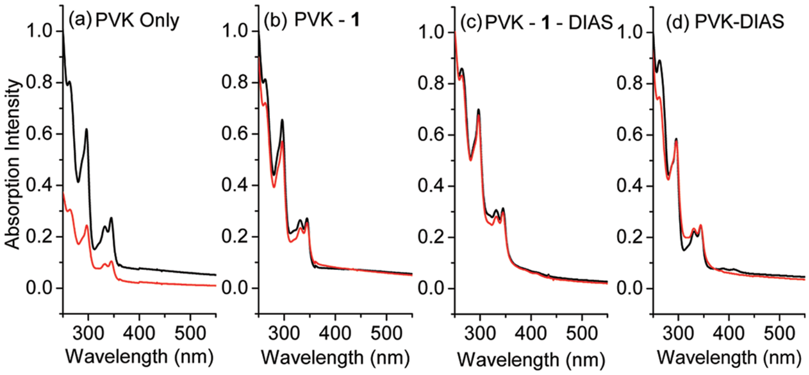

Figure 3. Photochemical activity of the PVK based materials. The change was monitored by UV−vis absorption spectra: (a) PVK: before irradiation (black line); after irradiation and development (red line). (b) PVK-**1**: before irradiation (black line); after irradiation and development (red line). (c) PVK-**1**-DIAS: before irradiation (black line); after irradiation and development (red line). (d) PVK-DIAS: before irradiation (black line); after irradiation and development (red line).

Another question to be addressed is the mechanism of the photochemical cross-linking process. One may wonder whether the TPA group or the *p*-benzylic acetate side-chains are the necessary part for inducing the cross-linking process. To address this question, we have adopted a blend of TPA in PVK as a model in the next experiment for comparison.

In the study, a film of PVK-TPA was subjected to photocuring and development as mentioned before. After the development, only around 50% of the film was found to be maintained on the substrate, illustrating that the presence of the TPA core alone does not bring in enough degree of cross-linking. Therefore, the presence of the *para*-benzylic acetate components on **1** is the key part to induce the cross-linking process.

To enhance the sensitivity of the photocuring process, PAG was employed in the third experiment. It has been reported that di and triphenylmethane dyes such as Leuco dyes or Michler's hydrol are sensitive toward acid-promoted dissociation.[15] Therefore, we decided to examine if PAG would help to promote the dissociation of **1** and accelerate the cross-linking process. After a series of screening, we employed DIAS as the PAG in our study. As shown in Scheme 2,[16] photoirradiation of DIAS produces H^+ that might catalyze the decomposition of **1**. The concept of using PAG for acid-generation has been demonstrated decades ago and led to a revolution on the photolithographic technology.[17]

In the PAG promoted experiment, a mixture of DIAS-**1**−PVK was spin-coated on a quartz substrate for examination. After UV-irradiation and development in CH_2Cl_2, the I_R/I_O values of 0.95, 0.92, and 0.97 were found at 345, 331, and 296 nm respectively in Figure 3c. The observation of the high I_R/I_O values implied that almost all of the DIAS-**1**-PVK film had been cross-linked onto the substrate. This result reflects the potentials of using the DIAS-**1**-PVK system as a photolithographic material for PLED applications. The slight drop of the optical intensity at 331 nm may due to some loss of the DIAS during the development process.

Although the detail mechanisms about the photo cross-linking process are not certain, one may reasonably propose that the Friedel−Crafts reaction actually operates in the polymer matrix. As shown in Scheme 3, the benzylic cations may be generated either through direct photochemical excitation of **1** or through the acid-catalyzed process. Electrophilic aromatic substitution on the PVK matrix would therefore occur, leading to a highly cross-linked and intractable material.

Scheme 2. DIAS as the Photo-Acid Generator

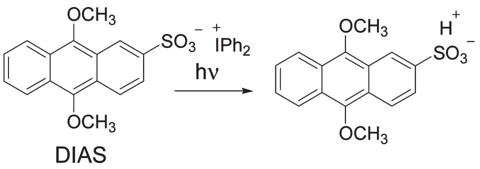

However, it is noteworthy to remember that several parallel mechanisms might operate simultaneously in the matrix. For example, Crivello had applied onium salt as photo initiator and PVK acted as photo sensitizer.[18] Equations in Scheme 4 show the mechanism about how the radical cations of the carbazole moieties were formed, which result in dimerization under UV-irradiation. The PVK would therefore begin to cross-link and become highly insoluble in organic solvents.

To probe this possibility, we have employed a DIAS-PVK blend to examine (Figure 3d). In the absence of **1**, the DIAS-PVK film could also be fully cross-linked on the substrate. The observation of almost identical I_R and I_O values at 345, 331, and 296 nm respectively, illustrating that the Crivello mechanism does operate in the present system and the DIAS could provide another pathway for the photochemical cross-linking process. The change of the spectral shape at 310−330 nm is due to the photodimerization of the carbazole unit. Similar change was observed in Figure 3a.

Evaluation of the Photochemical Reaction by ^1H NMR Study. To confirm whether the Friedel−Crafts type reactions would occur in the PVK matrix, we adopted 9-butyl-9H-carbazole (**6**) as a model to replace the PVK in the study. In this experiment, a **6**-**1**-DIAS blend, with the weight ratio of 48.4: 10: 1, was spin-coated on a quartz plate, and irradiated under Ar and postbaked as usual. The mole-ratio of **6**-**1**-DIAS in the film was estimated, according to their weight ratio, as 10: 1: 0.1, which is in good agreement with the ^1H NMR data shown in Figure 4a. After irradiation, the film was dissolved in DMSO-d_6 and analyzed by ^1H NMR spectroscopy (Figure 4b). In the spectrum, the characteristic signals of **1**, including the aromatic signals at 7.29 and 6.98 (u and t), the methylene signal at 5.01 ppm (v), and the acetoxy signal (w) at 2.05 ppm (Figure 4a), clearly disappear and new peaks at 3.99 ppm (a), 6.84 ppm (b), 7.13 ppm (c), 7.98 ppm (d), and 8.06 (e) were observed instead (Figure 4b). The

Scheme 3. Photoinduced Cross-Linking Reaction

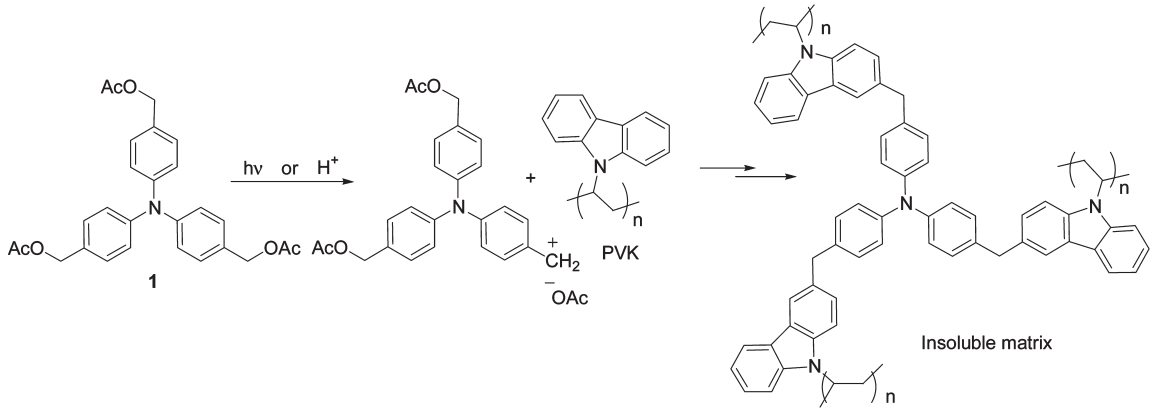

Scheme 4

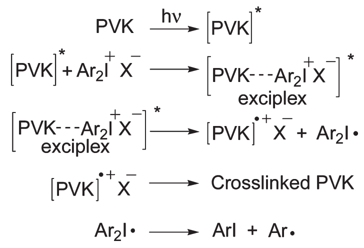

assignments are in good agreement with the ^{1}H NMR data of the authentic sample **7**, indicating that the Friedel−Crafts reactions do occur under the UV irradiation conditions. In particularly, the observation of the singlet signal at 3.99 ppm, a typical chemical shift for Ar−CH$_2$−Ar, strongly support the assumption about formation of the Friedel−Crafts product. According to the above observations, we propose that photoheterolytic cleavage would occur under UV irradiation to generate a benzyl cation intermediate that might undergo the Friedel−Crafts type coupling to give the cross-linking products. Having this promising preliminary result at hand, we started to focus our attention on the photoimageable polymer systems and their applications to PLED.

The use of 1 as the Photochemical Cross-Linker for PVK in PLED Applications. Although PVK is a known photoconductive material for Xerox application, the low-lying HOMO level, which leads to the high hole-injection barrier, usually hampers its potentials on PLED application.[19] Therefore, we are interested in investigating whether doping of **1** into PVK through photo cross-linking treatment would help to improve the hole-injection and transport properties. In the following experiments, we prepared the devices with the configuration of ITO/PVK-**1** (14 nm) /PVK-Ir(PPy)$_3$-PBD (75 nm)/Mg(2 nm)/Ag(100 nm), in which the amounts of **1** in PVK were varied in order to optimize conditions. Ir(PPy)$_3$, known as *fac*-tris(2-phenylpyridine)iridium, is an effective green phosphorescence emitter in PVK, while 2-(4-biphenyl)-5-(4-*tert*-butylphenyl)-1,3,4-oxadiazole (PBD) is an electron transporting material that has been widely used in this area.[8]

In this study, three types of PVK-**1** blends with different doping weight-percentages of 10, 20, and 40 of **1** respectively, were spin-coated onto the ITO glass substrate respectively, followed by UV-irradiation under Ar and postbaking treatments as described before. For convenience of the later discussion, the devices are named as PT10, PT20, and PT40 accordingly. The light emitting layer was then spin-coated, followed by vacuum deposition of a Mg/Ag cathode on top. The PLED device performances, including their brightness-voltage and current-efficiency-voltage behavior, were recorded and summarized in Table 2. Figure 5 presents the brightness-current efficiency-voltage relationships.

Having the lower doping ratio of **1** in PT10 and PT20, the hole-injection and transport properties of the PVK layer is relatively poor so that the corresponding PLED devices show higher turn-on voltage and lower maximum brightness. Nevertheless, PT20 demonstrates a great improvement on the device efficiency in comparison to that of PT10 so that the maximum current efficiency of 10 cd/A was achieved at 23.5 V. Under this condition, the brightness of 1320 cd/m^2 was recorded (Figure 5b). On the other hand, when the doping ratio of **1** in PVK was increased to 40% in PT40, the maximum electroluminescence of 5580 cd/m^2 and a much lower turn-on voltage of 15.5 V at 100 cd/m^2 were recorded, indicating that the hole injection and transport become largely improved. On the basis of these observations, we concluded that **1** not only played an important role in the cross-linking process but also contributes to the hole-injection and transport performance.

Use of PAG-1 as the Photochemical Cross-Linking Agent for PVK in PLED Applications. To enhance the efficiency of the photochemical cross-curing process, we adopted DIAS as the PAG to effect the Friedel−Crafts cross-coupling reactions. In the present study, a mixture of PAG-**1**-PVK, with the weight ratio of 1: 1: 9 was used. The device, denoted as PT10-PAG10 in Table 2, was prepared according to the procedures described in the previous section. The brightness-current/efficiency-voltage relationships are demonstrated in Figure 6. In this experiment, one can clearly see that the performance of the PVK-Ir(PPy)$_3$-PBD device was largely improved, indicating that the PAG-**1**-PVK blend could provide an effective hole-injection and transport layer after photoirradiation. It is noteworthy to mention that the turn-on voltage was significantly reduced. The voltage at 100 cd/m^2 drops to 13 V, which is the lowest among the devices we tested. When compared to the current efficiency of the device of PT10, the current efficiency of the device of PT10-PAG10 is enhanced almost by 45%. We tentatively attributed these phenomena to the effective cross-linking process that could help not only to cross-link the PVK backbones but also effectively anchor

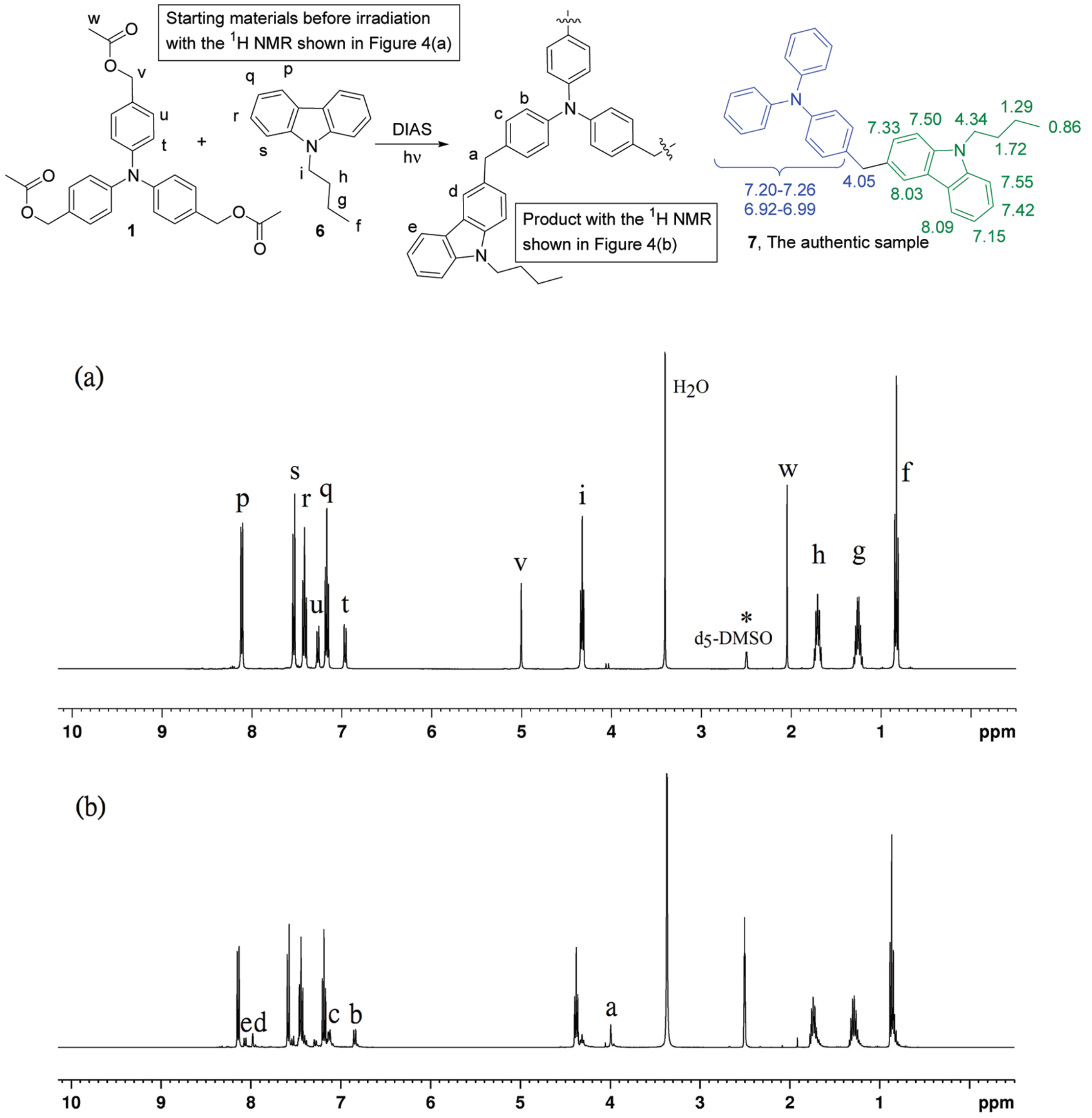

Figure 4. ^{1}H NMR of the products obtained by an acid-catalyzed cross-linker reaction of **1** and 9-butyl-carbazole (**6**) (1:10 mol-ratio): (a) before UV-irradiation; (b) after UV-irradiation.

Table 2. Electroluminescence Performance of the Devices of PT10, PT20, and PT40 in the Absence or Presence of PAG

device	voltage (V) at 100 cd·m^{-2}	max. brightness (cd·m^{-2}/V)	max. current efficiency (cd·A^{-1}/V)
PT10	19.5	3780/29	6.2/26
PT20	18.5	3450/28	10.0/23.5
PT40	15.5	5580/23.5	10.2/20
PT10-PAG10[a]	13	8220/20.5	9.0/16.5
PAG10	30	126/31	1.5/29.0

[a] The performance was comparable to that of the PEDOT:PSS modified standard device, which has a turn-on voltage of 12.5 V; with maximum brightness of 5036 cd/m^2 at 23 V.[8b]

the TPA components to the PVK matrix. In the absence of the PAG, the unreacted **1** would be leached out during the development process. Under this situation, high dopant ratio is required in order to have the PLED device with reasonable performance.

In the last experiments, a device of PAG10 was prepared from a mixture of DIAS-PVK (1:9). Although we have demonstrated in the previous section that DIAS is a good promoter to cross-link the PVK matrix, without help from the TPA components, the device shows extremely poor performance of high turn-on voltage and lower electroluminescence efficiency in the PLED applications.

Photolithographic Applications. As mentioned above, since DIAS-**1**-PVK could be effectively cross-linked onto the ITO substrate and become insoluble in CH_2Cl_2 after being subjected to UV irradiation, one might perceive that DIAS-**1**-PVK could be used as a negative tone photolithographic materials for PLED applications. To answer this question, PLED devices of ITO/DIAS-**1**-PVK/PVK-Ir(PPy)$_3$-PBD/Mg/Ag was fabricated as shown in Figure 7, parts a−c. A DIAS-**1**-PVK blend (the HTL), with the weight ratio of 1: 1: 9, was spun onto the ITO glass. After

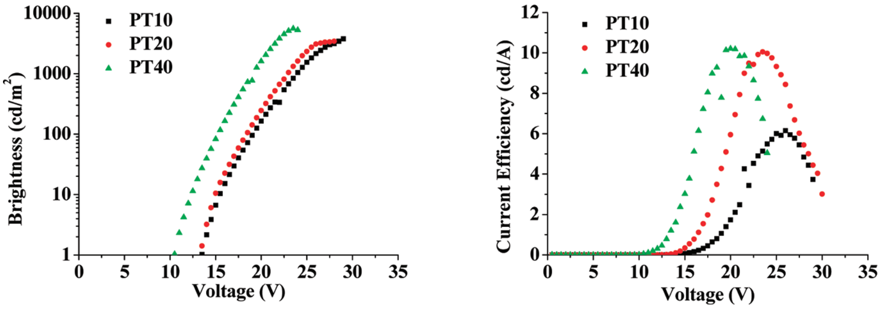

Figure 5. PLED performance of the devices of PT10, PT20, and PT40: (a) plots of brightness against voltage; (b) plots of current efficiency against voltage.

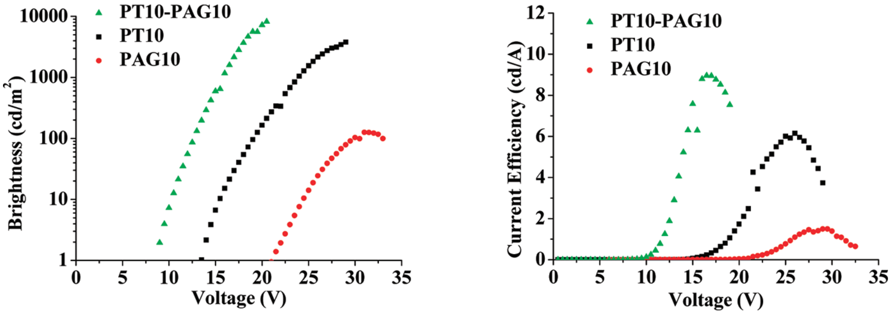

Figure 6. PLED performance of the devices of PT10, PT10-PAG10, and PAG10 for comparison: (a) plots of brightness against voltage; (b) plots of current-efficiency against voltage.

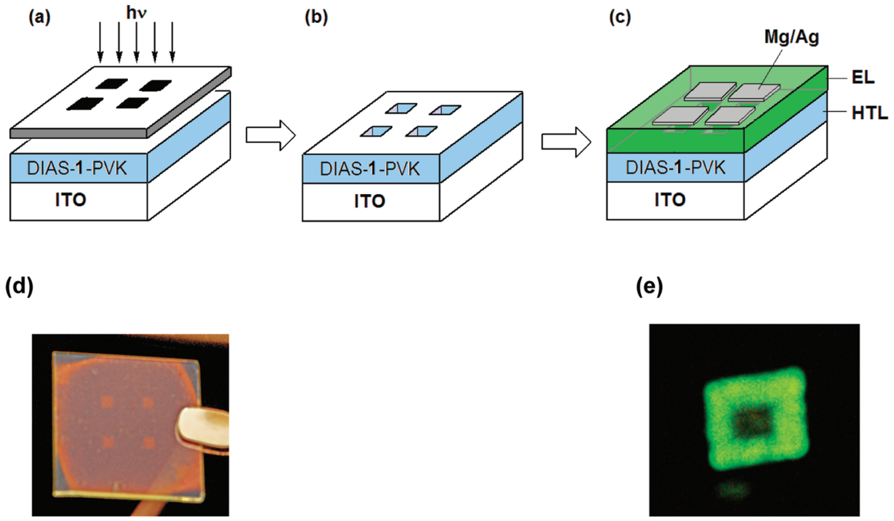

Figure 7. Fabrication of the DIAS-**1**-PVK based electroluminescence device: (a) The DIAS-**1**-PVK layer was exposed to UV-irradiation through a photomask with the four-dark-square pattern. (b) After development, the unexposed regions were dissolved and removed from the ITO substrated. (c) The EL layer and the Mg/Ag cathode were added on top to form the PLED. (d) A four-square image can be clearly observed after the PVK-Ir(PPy)$_3$-PBD was spun on top. (e) An electroluminescenc pattern of the PLED device was observed under the applied electrical voltage of 15 V. Each dark square has the surface area of 2 mm ×2 mm. The light emissive square, defined by the metallic cathode, has the surface area of 5 mm ×5 mm.

prebaking at 80 °C for 5 min, the DIAS-**1**-PVK-containing ITO was irradiated through a photomask, which has four dark squares (2 mm ×2 mm) on it, for 6 min under Ar. After development in CH_2Cl_2, the un-cross-linked polymers in the unexposed areas could be dissolved and removed. (Figure 7b). The layer of PVK-Ir(PPy)$_3$-PBD was then spin-coated on top. The position of the unexposed darker squares, as shown in Figure 7d, could be clearly differentiated due to their color difference. The Mg and Ag cathode was finally deposited by vapor deposition under high vacuum through a four-square shadow mask, with the size of 5 × 5 mm^2 for each square (Figure 7(c)). Because of the effective hole-transport properties of the retained DIAS-**1**-PVK layer, the exposed area exhibited a lower turn-on voltage. Therefore, the peripheral area can be selectively turned on while the central square (2 mm × 2 mm) still remains dark (Figure 7e) at 15 V.

CONCLUSIONS

In summary, we reported the use of DIAS-**1**-PVK as a useful photolithographic hole-injection and transport layer for PLED applications. Three parallel mechanisms, including the photo self-dimerization of the carbazole units, the Crivello onium salt sensitization mechanism and the photoacid catalyzed Friedel—Crafts type electrophilic aromatic substitutions were evidenced in the photocross-linking process. It is noteworthy to emphasize herein about the importance of the Crivello onium salt sensitization mechanism. Crivello has reported that the photohavesting function of the PVK matrix could help to sensitize the decomposition of the onium salt. On one hand, this will enable the direct cross-linking of the PVK matrix through the formation of the carbazole radical cations. On the other hand, photogenerated acid will help to catalyze the dissociation of **1** to generate the benzylic cationic species. Friedel—Crafts type electrophilic aromatic substitutions would then occur, anchoring the TPA units onto the PVK matrix. This will also lead to the further cross-linking of the PVK matrix. The operation of this duo process mechanism would lead to the photocross-linking with high efficiency. Through these reactions, the TPA cores could be tightly attached on the PVK backbone and will not leach out when being washed with CH_2Cl_2. The electronic properties, including the modified hole-injection barrier and the transport rate, could be reflected on the enhanced brightness (8220 cd m^{-2}), current efficiency (9.0 cd A^{-1} at 16.5 V), and the lowered turn-on voltage (13 V). The present study also demonstrated that the DIAS-**1**-PVK could be patterned by photolithographic techniques. By using a UV-photomask technique, the pattern image could be transferred onto the hole-transport layer. This technique may be beneficial for future PLED applications.

EXPERIMENTAL SECTION

Preparation of 4. Phosphorus oxychloride (37.4 mL) was added dropwise at 0 °C under Ar to DMF (40.8 mL) and the reaction mixture was stirred for 1 h. Triphenylamine (10.0 g) was added, and the resulting mixture was stirred at 105 °C for 4 h. After cooling to room-temperature, the mixture was poured into ice—water slowly, whereby a brown solid precipitated out. The solid was filtered, washed with water. The crude product was purified by column chromatography (CH_2Cl_2/Hex =1: 3) to yield **3** (10.0 g, 81%) as a yellow solid. Mp: 142—143 °C. ^{1}H NMR (400 MHz, acetone-d_6): δ 9.94 (s, 2H), 7.87 (t, J = 8.6 Hz, 4H), 7.49 (t, J = 7.86 Hz, 2H), 7.33 (t, J = 7.42 Hz, 1H), 7.23—7.27 (m, 6H). ^{13}C NMR (100 MHz, acetone-d_6): δ 191.07, 152.82, 146.61, 132.52, 131.87, 131.06, 128.04, 127.07, 123.56. HRMS (FAB): calcd for $C_{20}H_{15}NO_2$, 301.1103 (M^+); obsd, 301.1100. The dialdehyde **3** (10.0 g) was added on an ice-cooled mixture of $POCl_3$ (37.4 mL) in DMF (40.8 mL). The resulting mixture was reacted at 105 °C for 1 h. After reaction, the mixture was cooled to room-temperature and poured into ice—water slowly, whereby a brown solid precipitated out. The solid was collected by filtration and washed with water. The crude product was purified by column chromatography (CH_2Cl_2/Hex = 1:1) to yield **4** (4.0 g, 38%) as a bright yellow solid. Mp: 233—235 °C. ^{1}H NMR (400 MHz, acetone-d_6): δ 10.00 (s, 3H), 7.94 (d, J = 8.7 Hz, 6H), 7.36 (d, J = 8.7 Hz, 6H). ^{13}C NMR (100 MHz, acetone-d_6): δ 191.31, 152.14, 133.73, 132.04, 125.48. HRMS (FAB): calcd for $C_{21}H_{15}NO_3$, 329.1052 (M^+); obsd, 329.1053.

Preparation of 5. To the solution of the trialdehyde **4** (1.0 g) in ethanol (15.4 mL) was added sodium boron hydride (0.46 g) slowly at 0 °C. The ice bath was removed and the reaction was allowed to stir at room-temperature for 3 h. The ethanol was evaporated. The product was extracted with EtOAc and water. The organic extracts was collected and dried over anhydrous $MgSO_4$. The extracts was concentrated by rotary evaporation to yield **5** (0.9 g, 88%) as a white solid. Mp: 146—147 °C. ^{1}H NMR (400 MHz, acetone-d_6): δ 7.27 (d, J = 8.4, Hz, 6H), 6.99 (d, J = 8.4 Hz, 6H), 4.58 (d, J = 5.8 Hz, 6H), 4.12 (t, J = 5.8 Hz, 3H). ^{13}C NMR (100 MHz, acetone-d_6): δ 147.69, 137.82, 128.61, 124.47, 64.34. HRMS (FAB): calcd for $C_{21}H_{21}NO_3$, 335.1521 (M^+); obsd, 335.1520.

Preparation of 1. *To* a solution of **5** (1.0 g) in acetic anhydride (5 mL), diisopropylethylamine (1.56 mL) was added dropwise at 0 °C. The ice bath was the removed and the reaction was allowed to react at 40 °C for 2 h. After the reaction was complete, the mixture was cooled to room-temperature and poured into slurry of ice—water and ethyl acetate slowly. The excess acetic anhydride was hydrolyzed for 15 min. The residue was first exacted with HCl (5%) to remove diisopropylethylamine, followed by excess KOH (5%) to remove acetic acid, the side product. The organic layer was extracted, washed with brine, and dried over anhydrous $MgSO_4$, and concentrated by rotary evaporation to yield **1** (1.3 g, 94%) as yellow oil. Mp: 72—73 °C. ^{1}H NMR (400 MHz, DMSO-d_6): δ 7.29 (d, J = 8.44 Hz, 6H), 6.98 (d, J = 8.44 Hz, 6H), 5.00 (s, 6H), 2.05 (s, 9H). ^{13}C NMR (100 MHz, DMSO-d_6): δ 170.27, 146.78, 130.68, 129.73, 123.58, 65.15, 20.74. HRMS (FAB): calcd for $C_{27}H_{27}NO_6$, 461.1838 (M^+); obsd, 461.1829.

Preparation of 7. To a solution of **10** (0.1 g, 0.315 mmol) and excess **6** (0.7 g, 3.14 mmol) in $CHCl_3$ (1.6 mL), was added HCl (35%, 0.05 mL) dropwise at room temperature. The reaction was heated at 50 °C for 24 h. Water was added to quench the reaction. The product was exacted with $CHCl_3$ (2 × 10 mL). The organic extracts were dried over anhydrous $MgSO_4$ and concentrated by using rotary evaporation to give the crude product that was further purified by column chromatography on silica gel (CH_2Cl_2: Hex = 1:10) to yield **7** (0.04 g, 29%). ^{1}H NMR (400 MHz, DMSO-d_6): δ 8.09 (d, J = 7.7 Hz, 1H), 8.03 (s, 1H), 7.55 (d, J = 8.2 Hz, 1H), 7.50 (d, J = 8.3 Hz, 1H), 7.42 (m, 1H), 7.33 (d, J = 8.3 Hz, 1H), 7.26—7.20 (m, 6H), 7.15 (m, 1H), 6.99—6.92 (m, 8H), 4.34 (t, J = 7.02, Hz, 2H), 4.05 (s, 2H), 1.72 (q, J = 7.14, Hz, 2H), 1.33—1.24 (m, 2H), 0.86 (t, J = 7.36, Hz, 3H). ^{13}C NMR (100 MHz, DMSO-d_6): δ 147.36, 145.01, 140.26, 138.61, 137.32, 131.55, 129.64, 129.39, 126.76, 125.56, 124.35, 123.26, 122.50, 122.16, 121.85, 120.19, 120.08, 118.45, 109.23, 109.17, 42.01, 40.62, 30.72, 19.81, 13.72. HRMS (ESI): calcd for $C_{35}H_{32}N_2$, 480.64 (M^+); obsd, 480.50.

General Procedures for the EL Device Fabrication. The solution of the photoimageable hole transport material in $CHCl_3$ was spin-coated (3000 r.p.m., 60s) on a piece of precleaned ITO. The film obtained was baked at 80 °C for 5 min in order to remove any residual solvent. The ITO plate was covered with a piece of quartz mask and placed in Ar chamber for UV irradiation (17 mW, < 260 nm). After 6 min of photocuring, the ITO plate was postbaked at 130 °C for 5 min. The plate was then developed by immersion into CH_2Cl_2 for 10 s. The developed plate was dried at 80 °C for 5 min, followed by spin-coating of the EL layer (3000 rpm, 90 s) on top. The plate was then dried again at 80 °C for 5 min and send to the vacuum chamber for metal deposition. The pressure being used for vapor deposition was 5 × 10^{-6}. The deposition rate was 1 Å/s with the thickness of 20 Å for Mg. The deposition rate was 4 Å/s with the thickness of 1000 Å for Ag.

ASSOCIATED CONTENT

Ⓢ **Supporting Information.** NMR spectra, UV—vis spectrum, and plot of the heat treatment of **1**, and additional synthetic data. This material is available free of charge via the Internet at http://pubs.acs.org.

AUTHOR INFORMATION

Corresponding Author

*E-mail: mkleung@ntu.edu.tw.

ACKNOWLEDGMENT

The present work was supported by the Ministry of Education and National Taiwan University, National Science Council of Taiwan (NSC-98-2119-M-002-006-MY3 and 99-2119-M-002-007), and the thematic project, Academia Sinica.

REFERENCES

(1) (a) Tang, C. W.; Vanslyke, S. A. *Appl. Phys. Lett.* **1987**, *51*, 913–915. (b) Shen, Z.; Burrows, P. E.; Bulović, V.; Forrest, S. R.; Thompson, M. E. *Science* **1997**, *276*, 2009–2011.

(2) (a) Huang, J.; Su, J.-H.; Li, X.; Lam, M.-K.; Fung, K.-M.; Fan, H.-H.; Cheah, K.-W.; Chen, C. H.; Tian, H. *J. Mater. Chem.* **2011**, *21*, 2957–2964. (b) Chen, C.-H.; Huang, W.-S.; Lai, M.-Y.; Tsao, W.-C.; Lin, J. T.; Wu, Y.-H.; Ke, T.-H.; Chen, L.-Y.; Wu, C.-C. *Adv. Funct. Mater.* **2009**, *19*, 2661–2670. (c) Huang, T.-H.; Jiann, T.; Lin, J. T.; Chen, L.-Y.; Lin, Y.-T.; Wu, C.-C. *Adv. Mater.* **2006**, *18*, 602–606. (d) Burroughes, J. H.; Bradley, D. D. C.; Brown, A. R.; Marks, R. N.; Mackay, K.; Friend, R. H.; Burns, O. L.; Holmes, A. B. *Nature* **1990**, *347*, 539–541.

(3) (a) Sasabe, H.; Kido, J. *Chem. Mater.* **2011**, *23*, 621–630. (b) Koech, P. K.; Padmaperuma, A. B.; Wang, L.; Swensen, J. S.; Polikarpov, E.; Darsell, J. T.; Rainbolt, J. E.; Gaspar, D. J. *Chem. Mater.* **2010**, *22*, 3926–3932. (c) Li, J.; Ma, C.; Tang, J.; Lee, C.-S.; Lee, S. *Chem. Mater.* **2005**, *17*, 615–619. (d) Kulkarni, A. P.; Tonzola, C. J.; Babel, A.; Jenekhe, S. A. *Chem. Mater.* **2004**, *16*, 4556–4753. (e) Kim, Y.; Bae, K. H.; Jeong, Y. Y.; Choi, D. K.; Ha, C.-S. *Chem. Mater.* **2004**, *16*, 5051–5057.

(4) (a) Ko, L.-C.; Liu, T.-Y.; Chen, C.-Y.; Yeh, C.-L.; Tseng, S.-R.; Chao, Y.-C.; Meng, H.-F.; Lo, S.-C.; Burn, P. L.; Horng, S.-F. *Org. Electron.* **2010**, *11*, 1005–1009. (b) Chong, L.-W.; Lee, Y.-L.; Wen, T.-C.; Guo, T.-F. *Appl. Phys. Lett.* **2006**, *89*, 233513.

(5) For recent review, see: Zhong, C.; Duan, C.; Huang, F.; Wu, H.; Cao, Y. *Chem. Mater.* **2011**, *23*, 326–340. For other examples, see: (a) Lin, K.-R.; Chang, C.-C.; Chang Chien, Y.-H.; Leung, M.-k.; Liu, S.-W.; Lee, J.-H.; Hsieh, K.-H.. *Langmuir* **2010**, *26*, 5147–5152. (b) Wallikewitz, B. H.; Hertel, D.; Meerholz, K. *Chem. Mater.* **2009**, *21*, 2912–2919. (c) Li, J.; Marks, T. J. *Chem. Mater.* **2008**, *20*, 4873–4882. (d) Ma, B.; Lauterwasser, F.; Deng, L.; Zonte, C. S.; Kim, Z. B.; Fréchet, J. M. J.; Borek, C.; Thompson, M. E. *Chem. Mater.* **2007**, *19*, 4827–4832. (e) Tsai, L.-R.; Chen, Y. *J. Polym. Sci., Part A: Polym. Chem.* **2008**, *46*, 70–84. (f) Tang, D.-F.; Wen, G.-A.; Qi, X.-Y.; Wang, H.-Y.; Peng, B.; Wei, W.; Huang, W. *Polymer* **2007**, *48*, 4412–4418. (g) Jungermann, S.; Riegel, N.; Müller, D.; Meerholz, K.; Nuyken, O. *Macromolecules* **2006**, *39*, 8911–8919. (h) Bacher, E.; Bayerl, M.; Rudati, P.; Reckefuss, N.; Müller, C. D.; Meerholz, K.; Nuyken, O. *Macromolecules* **2005**, *38*, 1640–1647. (i) Yan, H.; Lee, P.; Armstrong, N. R.; Graham, A.; Evmenenko, G. A.; Dutta, P.; Marks, T. J. *J. Am. Chem. Soc.* **2005**, *127*, 3172–3183. (j) Yan, H.; Scott, B. J.; Huang, Q.; Marks, T. J. *Adv. Mater.* **2004**, *16*, 1948–1952. (k) Müller, C. D.; Falcou, A.; Reckefuss, N.; Rojahn, M.; Wiederhirn, V.; Rudati, P.; Frohne, H.; Nuyken, O.; Becker, H.; Meerholz, K. *Nature* **2003**, *421*, 829–833.

(6) (a) Gates, B. D.; Xu, Q.; Stewart, M.; Ryan, D.; Willson, C. G.; Whitesides, G. M. *Chem. Rev.* **2005**, *105*, 1171–1196. (b) Amos, F. F.; Morin, S. A.; Streifer, J. A.; Hamers, R. J.; Jin, S. *J. Am. Chem. Soc.* **2007**, *129*, 14296–14302. (c) Salavagione, H. J.; Miras, M. C.; Barbero, C. *Macromol. Rapid Commun.* **2006**, *27*, 26–30. (d) Schanze, K. S.; Bergstedt, T. S.; Hauser, B. T. *Adv. Mater.* **1996**, *8*, 531–534. (e) Yamada, S.; Mrozek, T.; Rager, T.; Owens, J.; Rangel, J.; Willson, C. G.; Byers, J. *Macromolecules* **2004**, *37*, 377–384. (f) Lee, S. K.; Jung, B. J.; Ahn, T.; Song, I.; Shim, H.-K. *Macromolecules* **2003**, *36*, 9252–9256.

(7) (a) Cho, M. J.; Shin, J.; Jin, J.-I.; Kim, Y. M.; Park, Y. W.; Ju, B.-K.; Choi, D. H. *Synth. Met.* **2009**, *159* (19−20), 2147–2152. (b) Jiang, G.; Baba, A.; Advincula, R. C. *Langmuir* **2007**, *23*, 817–825. (c) Briseno, A. L.; Roberts, M.; Ling, M.-M.; Moon, H.; Nemanick, E. J.; Bao, Z. *J. Am. Chem. Soc.* **2006**, *128*, 3880–3881. (d) Jegadesan, S.; Sindhu, S.; Advincula, R. C.; Valiyaveettil, S. *Langmuir* **2006**, *22*, 780–786. (e) Jegadesan, S.; Advincula, R. C.; Valiyaveettil, S. *Adv. Mater.* **2005**, *17*, 1282–1285. (f) Xia, C.; Advincula, R. C.; Baba, A.; Knoll, W. *Chem. Mater.* **2004**, *16*, 2852–2856.

(8) (a) Chang, C.-C.; Leung, M.-k. *Chem. Mater.* **2008**, *20*, 5816–5821. (b) Lin, K.-R.; Chang Chien, Y.-H.; Chang, C.-C.; Hsieh, K.-H.; Leung, M.-k. *Macromolecules* **2008**, *41*, 4158–4164. (c) Ku, C.-H.; Kuo, C.-H.; Chen, C.-Y.; Leung, M.-k.; Hsieh, K.-H. *J. Mater. Chem.* **2008**, *18*, 1296–1301. (d) Chiang, C. C.; Chen, H.-C.; Lee, C.-s.; Leung, M.-k.; Lin, K.-R.; Hsieh, K.-H.. *Chem. Mater.* **2008**, *20*, 540–552. (e) Chou, M.-Y.; Leung, M.-k.; Su, Y. O.; Chiang, C. L.; Lin, C.-C.; Liu, J.-H.; Kuo, C.-K.; Mou, C.-Y. *Chem. Mater.* **2004**, *16*, 654–661. (f) Leung, M.-k.; Chou, M.-Y.; Su, Y. O.; Chiang, C. L.; Chen, H.-L.; Yang, C. F.; Yang, C.-C.; Lin, C.-C.; Chen, H.-T. *Org. Lett.* **2003**, *5*, 839–842.

(9) For review, see: (a) Shirota, Y. *J. Mater. Chem.* **2000**, *10*, 1. For other examples, see: (b) Kimoto, A.; Cho, J. S.; Higuchi, M.; Yamamoto, K. *Macromolecules* **2004**, *37*, 5531–5537. (c) Thomas, K. R. J.; Lin, J. T.; Tao, Y.-T.; Ko, C. W. *Adv. Mater.* **2000**, *12*, 1949–1951. (d) Thomas, K. R. J.; Lin, J. T.; Tao, Y.-T.; Ko, C. W. *J. Am. Chem. Soc.* **2001**, *123*, 9404–9411. (e) Bach, U.; De Cloedt, K.; Spreitzer, H.; Grätzel, M. *Adv. Mater.* **2000**, *12*, 1060–1063.

(10) (a) Malwa, H. S. *Handbook of Advanced Electronic and Photonic Materials and Devices*; Academic: San Diego, CA, 2001; Vol. 10. (b) Adachi, C.; Tsutsui, T.; Saito, S. *Appl. Phys. Lett.* **1990**, *57*, 531–533.

(11) For recent reviews, see: (a) Boudreault, P.-L. T.; Beaupre, S.; Leclerc, M. *Polym. Chem.* **2010**, *1*, 127–136. (b) Boudreault, P.-L. T.; Blouin, N.; Leclerc, M. *Adv. Polym. Sci.* **2008**, *212*, 99–124. (c) Blouin, N.; Leclerc, M. *Acc. Chem. Res.* **2008**, *41*, 1110–1119.(d) Yang, X.-H.; Jaiser, F.; Neher, D. *Highly Efficient OLEDs with Phosphorescent Materials*; Yersin, H., Ed.; Wiley-VCH: Weinheim, 2008; pp 221−258. For other examples, see: (a) Thomas, J.; Christenson, C. W.; Blanche, P.-A.; Yamamoto, M.; Norwood, R. A.; Peyghambarian, N. *Chem. Mater.* **2011**, *23*, 416–429. (b) Zhang, K.; Tao, Y.; Yang, C.; You, H.; Zou, Y.; Qin, J.; Ma, D. *Chem. Mater.* **2008**, *20*, 7324–7331. (c) Fulghum, T. M.; Taranekar, P.; Advincula, R. C. *Macromolecules* **2008**, *41*, 5681–5867. (d) Inaoka, S.; Roitman, D. B.; Advincula, R. C. *Chem. Mater.* **2005**, *17*, 6781–6789. (e) Nakamura, A.; Tada, T.; Mizukami, M.; Hirose, S.; Yagyu, S. *Appl. Phys. Lett.* **2002**, *80*, 2189–2191. (f) Moisan, J. Y.; Andre, B.; Lever, R. *Chem. Phys.* **1991**, *153* (1−2), 305–312.

(12) Mallegol, T.; Gmouh, S.; Meziane, M. A. A.; Blanchard-Desce, M.; Mongin, O. *Synthesis* **2005**, *11*, 1771–1774.

(13) Bussiere, P.-O.; Mailhot, B.; Rivaton, A.; Barthe, M.-F.; Gardette, J.-L.; Baba, M. *Polym. Degrad. Stab.* **2008**, *93*, 1376–1382.

(14) Rivaton, A.; Mailhot, B.; Derderian, G.; Bussiere, P. O.; Gardette, J.-L. *Macromolecules* **2003**, *36*, 5815–5824.

(15) (a) Sinha, S. K.; Katiyar, S. S. *J. Phys. Chem.* **1970**, *74*, 1382–1388. (b) Biddle, H. C.; Porter, C. W. *J. Am. Chem. Soc.* **1915**, *37*, 1571–1589.

(16) Cupta, M. G.; Joseph, P., J.; Kohl, P. A. *J. Appl. Polym, Sci.* **2007**, *105*, 2655–2662.

(17) (a) Reichmanis, E.; Thompson, L. F. *Chem. Rev.* **1989**, *89*, 1273–1289. (b) Reichmanis, E.; Nalamasu, O.; Houlihan, F. M. *Acc. Chem. Res.* **1999**, *32*, 659–667.

(18) (a) Hua, Y.; Crivello, J. V. *Macromolecules* **2001**, *34*, 2488–2494. (b) Crivello, J. V. *J. Photopolym. Sci. Technol.* **2009**, *22*, 575–582.

(19) Partridge, R. H. *Polymer* **1983**, *24*, 739–747.